Inorganic Chemistry

ARTICLE

pubs.acs.org/IC

# Analysis of the Photomagnetic Properties of Cyano-Bridged Heterobimetallic Complexes by X-Ray Diffraction

Helle Svendsen,[†] Mads Ry Vogel Jørgensen,[†] Jacob Overgaard,[†] Yu-Sheng Chen,[‡] Guillaume Chastanet,[§] Jean-François Létard,[§] Kenichi Kato,[∥] Masaki Takata,[∥] and Bo B. Iversen*[,†]

[†]Centre for Materials Crystallography, Department of Chemistry and iNANO, Aarhus University, DK-8000 Århus C, Denmark

[‡]ChemMatCARS beamline, The University of Chicago, Advanced Photon Source, Argonne, Illinois 60439, United States

[§]CNRS, Université de Bordeaux, ICMCB, 87 avenue du Dr. A. Schweitzer, Pessac, F-33608, France

[∥]RIKEN SPring-8 Center, 1-1-1 Kouto, Sayo-cho, Sayo-gun, Hyogo 679-5148, Japan

Supporting Information

**ABSTRACT:** Single crystal synchrotron X-ray diffraction measurements have been carried out on $[Nd(DMF)_4(H_2O)_3(\mu\text{-}CN)Fe(CN)_5]\cdot H_2O$ (DMF = dimethyl-formamide), **1**; $[Y(DMF)_4(H_2O)_3(\mu\text{-}CN)Fe(CN)_5]\cdot H_2O$, **2**; $[Ce(DMF)_4(H_2O)_3(\mu\text{-}CN)Fe(CN)_5]\cdot H_2O$, **3**; $[Sm(DMF)_4(H_2O)_3(\mu\text{-}CN)Fe(CN)_5]\cdot H_2O$, **4**; $[Tb(DMF)_4(H_2O)_3(\mu\text{-}CN)Fe(CN)_5]\cdot H_2O$, **5**; $[Yb(DMF)_4(H_2O)_3(\mu\text{-}CN)Fe(CN)_5]\cdot H_2O$, **6**; and $[Nd(DMF)_4(H_2O)_3(\mu\text{-}CN)Co(CN)_5]\cdot H_2O$, **7**, at 15(2) K with and without UV illumination of the crystals. Significant changes in unit cell parameters are observed for all of the iron-containing complexes, while compound **7** shows no response to UV illumination. These results are consistent with previous results and are furthermore reproduced by powder synchrotron X-ray diffraction for compounds **1** and **7**. Photoexcited crystal structures have been determined for **1**−**6** from refinements of two-conformer models, and excited state occupancies in the range 80−94% are found. Significant bond length changes are observed for the Fe−ligand bonds (up to 0.06 Å), the cyano bonds (up to 0.02 Å), and the lanthanide−ligand bonds (up to 0.1 Å). On the contrary, powder X-ray diffraction on the simple compound $K_3Fe(CN)_6$, **8**, upon UV illumination does not show any structural changes, suggesting that the photomagnetic effect requires the presence of both the transition metal and the lanthanide ion. Photomagnetic measurements show an increase in magnetization of the excited state of **1** of up to 3%, which is much diminished compared with previously published values of 45%. Furthermore, they show that the isostructural complex $[La(DMF)_4(H_2O)_3(\mu\text{-}CN)Fe(CN)_5]\cdot H_2O$, **9**, exhibits identical magnetic responses in the UV-induced excited crystal structure.

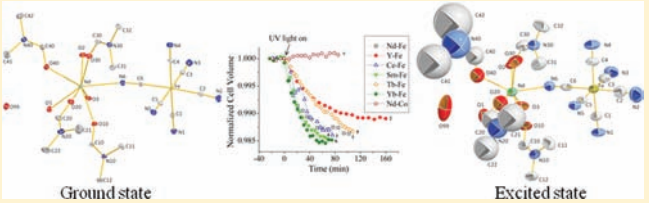


## INTRODUCTION

Photocrystallography offers a new and unique insight into the three-dimensional structure of excited state crystal structures of solid state materials and by now has become an evolving branch of modern crystallography.[1−6] Many different types of photoswitchable effects such as ligand isomerizations[7−11] and spin transitions[2,4,5,12−15] have been investigated using this technique without any need for time-resolution. Other photoexcited processes require time-resolved studies, and excited state crystal structures with lifetimes in the micro- and picosecond range have also been investigated using photocrystallography.[16−20]

Some photoexcited processes not only induce structural changes but are also accompanied by changes in the magnetic properties. This is, e.g., the case for Fe(II) spin transition compounds (LIESST process) where the number of unpaired spins is increased, leading to increases in the Fe−ligand bonds by as much as 0.2 Å.[1] In 2003, Li et al. published a study on a cyanide-bridged hetero-bimetallic complex containing neodymium and iron, $[Nd(DMF)_4(H_2O)_3(\mu\text{-}CN)Fe(CN)_5]\cdot H_2O$ (**1**, NdFeDMF; DMF = dimethyl-formamide), which exhibits a large increase of the magnetic susceptibility upon illumination with UV light at low temperatures ($T < \sim 50$ K).[21] The nature of the electronic transition, which causes the change in the magnetic properties in **1**, is unknown, but significant structural changes have been determined using a conventional very low temperature crystallographic technique, as the excited state of **1** is metastable with a lifetime of several hours at temperatures below 50 K.[21,22] The largest modifications were found in the $Fe(CN)_6$ moiety of the structure, which indicated that this part of the structure must play an important role in the excitation process. Two isostructural compounds and even a related compound without any cyanide link between the two metal centers have also shown similar changes in the $Fe(CN)_6$ enitity when illuminated with UV light.[23,24] This suggests that these compounds potentially also could exhibit photomagnetic properties, but their photomagnetic behavior upon light-illumination so far has not been probed. Photoinduced changes in the magnetization have been

**Received:** July 18, 2011
**Published:** October 10, 2011

**Table 1. Crystallographic Data and Refinement Residuals for 1−7**

| | NdFeDMF (**1**) | | YFeDMF (**2**) | | CeFeDMF (**3**) | |
|---|---|---|---|---|---|---|
| dat. col | GS | EXC | GS | EXC | GS | EXC |
| space group | $P2_1/n$ | $P2_1/n$ | $P2_1/c$ | $P2_1/c$ | $P2_1/n$ | $P2_1/n$ |
| $T$ (K) | 15(2) | 15(2) | 15(2) | 15(2) | 15(2) | 15(2) |
| $a$ (Å) | 17.5855(4) | 17.3813(3) | 13.8250(5) | 13.7568(7) | 17.6548(5) | 17.4053(5) |
| $b$ (Å) | 8.8160(2) | 8.7866(2) | 8.8075(3) | 8.7827(5) | 8.8494(2) | 8.8119(2) |
| $c$ (Å) | 19.4029(5) | 19.4646(4) | 24.4849(8) | 24.402(1) | 19.4348(5) | 19.5250(6) |
| $\beta$ (deg) | 96.241(2) | 96.7519(7) | 96.643(2) | 96.695(2) | 96.1540(7) | 96.4743(8) |
| $V$ (Å$^3$) | 2990.3(1) | 2952.1(1) | 2961.4(2) | 2928.2(3) | 3018.9(1) | 2975.5(1) |
| $\mu$ (mm$^{-1}$) | 0.47 | 0.47 | 0.56 | 0.56 | 0.43 | 0.43 |
| $N_{obs}$ | 203045 | 55465 | 142171 | 102097 | 91744 | 89119 |
| $N_{unique}$ | 45643 | 16046 | 43920 | 18436 | 23219 | 22874 |
| sin $\theta/\lambda_{max}$ | 1.296 | 0.982 | 1.268 | 0.984 | 1.062 | 1.059 |
| $R_{int}$ | 0.0767 | 0.0466 | 0.0674 | 0.0626 | 0.0526 | 0.0521 |
| $\langle\sigma(I)/I\rangle$ | 0.0688 | 0.0803 | 0.0768 | 0.0852 | 0.0691 | 0.1259 |
| $N_{obs}(2\sigma)$ | 32742 | 7969 | 31832 | 10075 | 16822 | 10557 |
| $N_{par}$ | 367 | 294 | 367 | 294 | 367 | 294 |
| $R_{all}$ | 0.0769 | 0.1428 | 0.0893 | 0.1564 | 0.072 | 0.1697 |
| $R(F)$ (2s) | 0.051 | 0.0639 | 0.0623 | 0.0825 | 0.0431 | 0.0663 |
| $R_w(F^2)$ (2$\sigma$) | 0.0951 | 0.113 | 0.138 | 0.1548 | 0.0734 | 0.1091 |
| GOF | 1.331 | 1.839 | 1.636 | 2.321 | 1.299 | 1.553 |
| occ | N/A | 0.8609(19) | N/A | 0.829(2) | N/A | 0.799(2) |
| | SmFeDMF (**4**) | | TbFeDMF (**5**) | | YbFeDMF (**6**) | |
| dat. col | GS | EXC | GS | EXC | GS | EXC |
| space group | $P2_1/n$ | $P2_1/n$ | $P2_1/c$ | $P2_1/c$ | $P2_1/c$ | $P2_1/c$ |
| $T$ (K) | 15(2) | 15(2) | 15(2) | 15(2) | 15(2) | 15(2) |
| $a$ (Å) | 17.6117(6) | 17.3433(5) | 13.8590(6) | 13.7713(4) | 13.8284(6) | 13.7301(4) |
| $b$ (Å) | 8.7894(3) | 8.7536(3) | 8.8290(4) | 8.7962(3) | 8.7914(4) | 8.7451(2) |
| $c$ (Å) | 19.3792(7) | 19.4798(7) | 24.532(1) | 24.4444(8) | 24.438(1) | 24.2878(7) |
| $\beta$ (deg) | 96.255(1) | 96.570(1) | 96.695(1) | 96.7654(9) | 96.693(1) | 96.5683(7) |
| $V$ (Å$^3$) | 2982.0(2) | 2937.9(2) | 2981.3(2) | 2940.5(2) | 2950.7(4) | 2897.1(1) |
| $\mu$ (mm$^{-1}$) | 0.43 | 0.43 | 0.62 | 0.62 | 0.81 | 0.81 |
| $N_{obs}$ | 90922 | 90136 | 89164 | 84936 | 82212 | 81684 |
| $N_{unique}$ | 23892 | 23650 | 20032 | 16115 | 15842 | 15583 |
| sin $\theta/\lambda_{max}$ | 1.06 | 1.063 | 1.061 | 0.983 | 0.905 | 0.904 |
| $R_{int}$ | 0.0594 | 0.0556 | 0.0702 | 0.0472 | 0.0708 | 0.0627 |
| $\langle\sigma(I)/I\rangle$ | 0.0661 | 0.1099 | 0.0683 | 0.0622 | 0.0667 | 0.0919 |
| $N_{obs}(2\sigma)$ | 17829 | 11645 | 15495 | 9880 | 12659 | 7802 |
| $N_{par}$ | 367 | 294 | 367 | 294 | 375 | 294 |
| $R_{all}$ | 0.0598 | 0.151 | 0.0607 | 0.1143 | 0.0539 | 0.1564 |
| $R(F)$ (2$\sigma$) | 0.0383 | 0.0638 | 0.0429 | 0.0629 | 0.039 | 0.073 |
| $R_w(F^2)$ (2$\sigma$) | 0.0689 | 0.1073 | 0.0901 | 0.1083 | 0.0679 | 0.1277 |
| GOF | 1.176 | 1.542 | 1.341 | 2.188 | 1.174 | 1.95 |
| occ | N/A | 0.842(2) | N/A | 0.867(2) | N/A | 0.942(2) |
| | | | NdCoDMF (**7**) | | | |
| dat. col | | | GS | | | EXC |
| space group | | | $P2_1/n$ | | | $P2_1/n$ |
| $T$ (K) | | | 15(2) K | | | 15(2) K |
| $a$ (Å) | | | 17.5359(5) | | | 17.5347(6) |
| $b$ (Å) | | | 8.7908(2) | | | 8.7967(3) |
| $c$ (Å) | | | 19.3874(5) | | | 19.4154(6) |


dx.doi.org/10.1021/ic2015258 |*Inorg. Chem.* 2011, 50, 10974–10984

**Table 1. Continued**

| | NdCoDMF (7) | |
|---|---|---|
| dat. col | GS | EXC |
| $\beta$ (deg) | 96.2279(6) | 96.2436(8) |
| $V$ (Å$^3$) | 2971.0(1) | 2977.0(2) |
| $\mu$ (mm$^{-1}$) | 0.498 | 0.498 |
| $N_{obs}$ | 86706 | 86909 |
| $N_{unique}$ | 15892 | 15953 |
| sin $\theta/\lambda_{max}$ | 0.906 | 0.905 |
| $R_{int}$ | 0.0592 | 0.0602 |
| $\langle\sigma(I)/I\rangle$ | 0.0382 | 0.0396 |
| $N_{obs}(2\sigma)$ | 15015 | 13799 |
| $N_{par}$ | 367 | 367 |
| $R_{all}$ | 0.0298 | 0.0335 |
| $R(F)$ $(2\sigma)$ | 0.0247 | 0.027 |
| $R_w(F^2)$ $(2\sigma)$ | 0.0568 | 0.0609 |
| GOF | 1.472 | 1.516 |

confirmed in only two other related complexes—$[Nd(DMF)_4(H_2O)_3(\mu\text{-}CN)Co(CN)_5]\cdot H_2O$ (**7**, NdCoDMF) and $[Nd(HP)_4(H_2O)_3(\mu\text{-}CN)Fe(CN)_5]\cdot H_2O$ (HP = 4-hydroxypyridine), both showing an enhancement in the magnetic susceptibility upon visible and UV light illumination, respectively.[25,26]

In an attempt to increase the excitation rate, new photocrystallographic experiments using synchrotron radiation have been performed for NdFeDMF (**1**) and six isostructural compounds. The high intensity of the X-ray beam facilitates the use of smaller crystals, which may increase the population of the excited state in the crystal after illumination. The results are compared with our earlier results obtained for NdFeDMF (**1**) performed at a conventional laboratory X-ray source diffractometer.[22] Furthermore, synchrotron powder diffraction experiments on NdFeDMF (**1**) and NdCoDMF (**7**) have also been performed in order to investigate whether higher excitation rates are achieved using another photocrystallographic setup, where the size of the crystallites is even smaller. The results are also correlated to photomagnetic measurements on **1** and **8**. Finally, a powder diffraction experiment was carried out for $K_3Fe(CN)_6$ upon UV illumination in order to investiage whether any structural changes appear in isolated $Fe(CN)_6^{3-}$ units.

## EXPERIMENTAL SECTION

**Synthesis.** The seven different compounds (NdFeDMF (**1**), YFeDMF (**2**), CeFeDMF (**3**), SmFeDMF (**4**), TbFeDMF (**5**), YbFeDMF (**6**), and NdCoDMF (**7**)) were synthesized by mixing $K_3[Fe(CN)_6]$ (or $K_3[Co(CN)_6]$ for **7**; 1 mmol) with water (10 mL). A lanthanide salt (1 mmol) dissolved in DMF (5 mL) was then added down the side of the glass very slowly. $LnCl_3$ was used for the Ln = Nd and Yb compounds, and $Ln(NO_3)_3$ was used for Ln = Y, Ce, Sm, and Tb, respectively. Green-yellow crystals precipitated, and crystals suitable for single crystal X-ray analysis were obtained after evaporation. The compounds NdFeDMF, CeFeDMF, SmFeDMF, and NdCoDMF are isostructural, crystallizing in the $P2_1/n$ space group, while YFeDMF, TbFeDMF, and YbFeDMF systems crystallize in the $P2_1/c$ space group. The crystal structures have identical molecular conformations as well as highly similar intermolecular contacts. All crystals have four molecular units ($[Ln(C_3H_7NO)_4Me(CN)_6]\cdot H_2O$) per unit cell. The molecules are connected to each other through hydrogen bonds formed by the crystal water molecules.

**Single Crystal X-Ray Diffraction.** Single crystal X-ray diffraction experiments with and without UV illumination were carried out at the ChemMatCARS beamline (ID-15) at the Advanced Photon Source, Argonne National Lab, Illinois, U.S.A. The data were measured at a Bruker D8 diffractometer equipped with a Bruker APEXII CCD detector. The crystals were cooled down to approximately 15 K by the use of a helium cryostat (Pinkerton type cooling device).[27] The crystals (~50 $\mu$m) were attached with oil on a goniometer head before being mounted on the diffractometer. A CUBE laser diode with a wavelength of 375 nm and a power output of 4 mW was used for the excitation of the samples. The diode was held fixed during the entire series of experiments, and the light was focused on the crystals by a lens. For each crystal, a ground state data set was measured (GS data collection), and only afterward was the UV light turned on. Identical small data collections of a few minutes were then repeated successively in order to determine the unit cell parameters as a function of time. When no further changes were observed in the cell parameter, a data collection identical to the GS data collection was repeated (EXC data collection)—also with continuous UV illumination. The data were integrated using the software SAINT+ and further processed and corrected for empirical absorption using SADABS.[28] The data were merged in SORTAV,[29] and the structures were refined with SHELXL-97.[28] All nonwater hydrogen atoms were refined as riding on the parent C atom. The GS data collection was refined using a single conformer with full occupancy on all sites. All atoms except hydrogen were treated anisotropically. The ground state fractional coordinates and atomic displacement parameters (ADPs) were then imported into the refinement of the EXC data collection, where two conformers were modeled: a refined excited state structure and a fixed ground state structure. The sum of their occupancies was constrained to unity, while restraints were imposed on the bond lengths in the DMF ligands of the excited state. All atoms except hydrogen in the excited state conformer were refined with anisotropic ADPs.

**Powder X-Ray Diffraction.** Photocrystallographic powder X-ray diffraction experiments were conducted at the BL44B2 beamline at SPring-8, Japan.[30] The experiments involved NdFeDMF (**1**) and NdCoDMF (**7**). The experimental setup has a Debye−Scherrer geometry with an image plate as the detector. The crystals were ground before being mounted in a 0.1 mm glass capillary. The sample was rotated

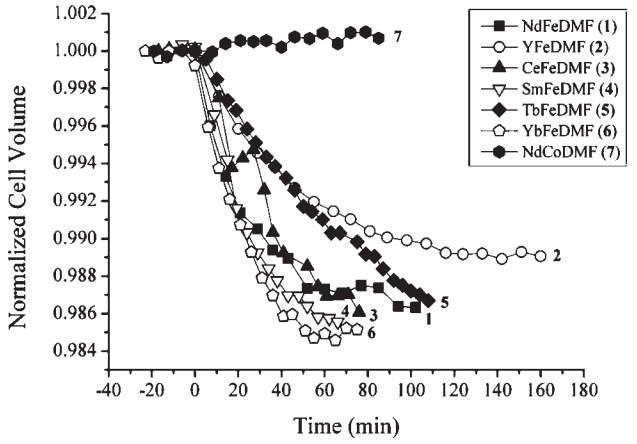


**Figure 1.** Unit cell volumes of **1**−**7** as a function of time determined by single-crystal X-ray diffraction. The laser is turned on immediately after $t = 0$ min. The complete excited state data collections took place after the last data point for each compound. The esd's are smaller than the symbols used in the plot.

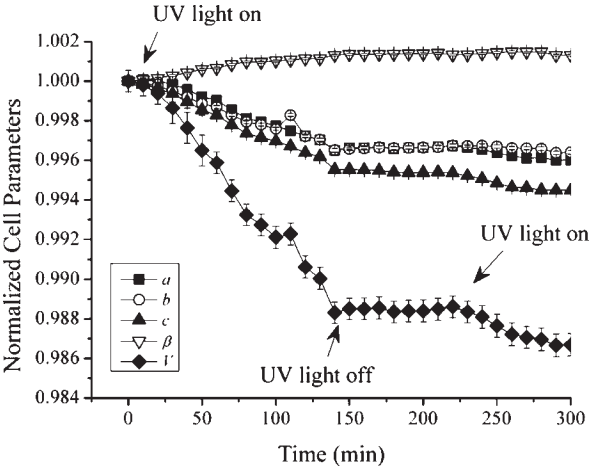


**Figure 2.** Unit cell volume of **1** (NdFeDMF) as a function of time determined by powder X-ray diffraction at 15 K. The laser is turned on immediately after $t = 0$ min, turned off at $t = 140$ min, and turned on again at $t = 240$ min.

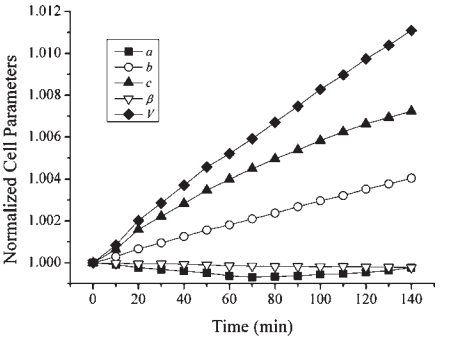


**Figure 3.** Unit cell volume of **7** (NdCoDMF) as a function of time determined by powder X-ray diffraction at 15 K. The laser is turned on immediately after $t = 0$ min. The esd's are smaller than the symbols used in the plot.

continuously during the experiments. A Helijet was used for cooling the sample down to approximately 15 K, while the same UV source as for the single-crystal experiments was used for illuminating the powder samples. A ground state data collection was measured before the UV or visible light was switched on, and several data collections were repeated.

The image plate data were converted into a one-dimensional diffractogram by the program IPV.[31] Due to insufficient data quality, Rietveld refinement of either ground state or excited state data collections was impossible on this large molecular complex. Instead, Le Bail fits have been performed for all data using Fullprof,[32] where only the cell parameters and zero point displacement were refined. The reliability factors were in the range of 3−5% for $R_p$ and 10−15% for $R_{wp}$.

**Magnetic Measurements.** Photomagnetic measurements were performed using the same CUBE Laser as used in the photocrystallographic measurements. The laser has a wavelength of 375 ± 5 nm coupled by means of an optical fiber to the cavity of a MPMS-5S Quantum Design SQUID magnetometer. The sample consists of a thin layer of powder placed 3 cm from the output of the optical fiber. The intensity was adjusted to obtain the best compromise between photomagnetic and warming effects.

## RESULTS AND DISCUSSION

Table 1 lists selected details from the crystallographic refinements. In Figure 1, the unit cell volumes normalized to the ground state values of **1**−**7** are plotted as a function of time upon UV illumination, i.e., before the complete excited state data collection.

A significant decrease in cell volume is observed for all of the Fe-containing compounds, **1**−**6**, when the UV light has been turned on. The largest decrease is observed for YbFeDMF (**6**), with a change in unit cell volume of 1.5%. Figure 1 shows that saturation has not been achieved for all complexes before the excited state data were measured. This is most evident for CeFeDMF (**3**) and TbFeDMF (**5**), where extrapolations of the unit cell volumes beyond the last data points suggest a continuing decrease. NdCoDMF (**7**) differs significantly from the rest of the compounds, as its unit cell volume is increasing slightly as function of time when illuminated with UV light. This is consistent with previous findings.[23]

The changes in unit cell parameters for NdFeDMF (**1**) and NdCoDMF (**7**) determined by the corresponding photocrystallographic powder diffraction experiments are plotted in Figures 2 and 3. Interestingly, it is seen in Figure 2 that when the UV irradiation was stopped, the unit cell did not recover to its original value. This provides further evidence that the evolution of the parameters is not due to an artificial thermal effect and that a real photoexcited state is populated. In addition, the fact that the unit cell decreases upon UV illumination rules out that the observed changes are merely due to heating.

For NdFeDMF (**1**), a significant decrease is observed for the cell axes $a$, $b$, and $c$, while $\beta$ increases. In total, these changes lead to a decrease of 1.3% in the unit cell volume. This is comparable to the changes obtained in the synchrotron single crystal experiment (Table 1 and Figure 1). Surprisingly, the powder experiment gives a decrease in the $c$ axis, while the single crystal results yield an increase. We have presently no explanation for this difference. In the case of NdCoDMF (**7**), only a slow increase in the cell volume is observed after turning on the UV light, which is consistent with the single crystal measurements.


dx.doi.org/10.1021/ic2015258 |*Inorg. Chem.* 2011, 50, 10974–10984

**Table 2. Metal−Ligand Bond Lengths and Cyanide Bond Lengths in the Ground State and the Excited State in 1−6 Including the Ratio and Percentage Change between the Ground State and Excited State Bond Lengths**

| | NdFeDMF (**1**) | | | | YFeDMF(**2**) | | | |
|---|---|---|---|---|---|---|---|---|
| bond | ground state (Å) | excited state (Å) | ratio | change (%) | ground state (Å) | excited state (Å) | ratio | change (%) |
| Fe−C1 | 1.924(1) | 1.907(5) | 0.991(3) | −0.9(3) | 1.9237(10) | 1.907(4) | 0.991(2) | −0.9(2) |
| Fe−C2 | 1.930(1) | 1.887(5) | 0.978(3) | −2.2(3) | 1.933(1) | 1.889(5) | 0.977(3) | −2.3(3) |
| Fe−C3 | 1.935(1) | 1.883(5) | 0.973(3) | −2.7(3) | 1.932(1) | 1.891(5) | 0.979(3) | −2.1(3) |
| Fe−C4 | 1.923(1) | 1.896(5) | 0.986(3) | −1.4(3) | 1.9222(10) | 1.883(4) | 0.980(2) | −2.0(2) |
| Fe−C5 | 1.9297(10) | 1.924(5) | 0.997(3) | −0.3(3) | 1.942(1) | 1.933(4) | 0.995(2) | −0.5(2) |
| Fe−C6 | 1.9325(10) | 1.904(5) | 0.985(3) | −1.5(3) | 1.921(1) | 1.896(4) | 0.987(2) | −1.3(2) |
| C1−N1 | 1.156(2) | 1.154(6) | 0.998(5) | −0.2(5) | 1.158(1) | 1.142(5) | 0.986(4) | −1.4(4) |
| C2−N2 | 1.157(2) | 1.180(7) | 1.02(6) | 2.0(6) | 1.159(2) | 1.173(6) | 1.012(5) | 1.2(5) |
| C3−N3 | 1.159(2) | 1.181(6) | 1.019(5) | 1.9(5) | 1.158(2) | 1.170(6) | 1.010(5) | 1.0(5) |
| C4−N4 | 1.1570(2) | 1.178(6) | 1.018(5) | 1.8(5) | 1.162(1) | 1.164(6) | 1.002(5) | 0.2(5) |
| C5−N5 | 1.158(1) | 1.149(5) | 0.992(4) | −0.8(4) | 1.162(1) | 1.149(5) | 0.989(4) | −1.1(4) |
| C6−N6 | 1.159(1) | 1.169(5) | 1.008(4) | 0.8(4) | 1.154(1) | 1.155(5) | 1.001(5) | 0.1(5) |
| X−N6 | 2.5390(9) | 2.465(4) | 0.971(2) | −2.9(2) | 2.4048(10) | 2.358(3) | 0.981(2) | −1.9(2) |
| X−O1 | 2.4546(9) | 2.471(4) | 1.007(2) | 0.7(2) | 2.3330(9) | 2.346(3) | 1.006(1) | 0.6(1) |
| X−O2 | 2.4441(8) | 2.435(3) | 0.996(1) | −0.4(1) | 2.3527(8) | 2.338(3) | 0.994(1) | −0.6(1) |
| X−O3 | 2.4744(8) | 2.472(3) | 0.999(1) | −0.1(1) | 2.3798(8) | 2.382(3) | 1.001(1) | 0.1(1) |
| X−O10 | 2.4108(8) | 2.400(3) | 0.996(1) | −0.4(1) | 2.3291(8) | 2.316(3) | 0.994(1) | −0.6(1) |
| X−O20 | 2.4269(8) | 2.444(5) | 1.007(2) | 0.7(2) | 2.3483(8) | 2.361(4) | 1.005(1) | 0.5(1) |
| X−O30 | 2.3939(9) | 2.394(4) | 1.000(2) | 0.0(2) | 2.3667(8) | 2.355(3) | 0.995(1) | −0.5(1) |
| X−O40 | 2.4402(9) | 2.510(5) | 1.029(2) | 2.9(2) | 2.3323(8) | 2.379(4) | 1.020(2) | 2.0(2) |
| | CeFeDMF(**3**) | | | | SmFeDMF(**4**) | | | |
| bond | ground state (Å) | excited state (Å) | ratio | change (%) | ground state (Å) | excited state (Å) | ratio | change (%) |
| Fe−C1 | 1.928(2) | 1.902(4) | 0.986(2) | −1.4(2) | 1.925(1) | 1.907(4) | 0.991(2) | −0.9(2) |
| Fe−C2 | 1.935(2) | 1.896(5) | 0.980(3) | −2.0(3) | 1.932(1) | 1.903(4) | 0.985(2) | −1.5(2) |
| Fe−C3 | 1.941(2) | 1.882(4) | 0.970(2) | −3.0(2) | 1.941(2) | 1.891(4) | 0.974(2) | −2.6(2) |
| Fe−C4 | 1.929(2) | 1.907(4) | 0.988(2) | −1.2(2) | 1.929(1) | 1.905(4) | 0.987(2) | −1.3(2) |
| Fe−C5 | 1.932(2) | 1.917(4) | 0.992(2) | −0.8(2) | 1.931(1) | 1.924(4) | 0.996(2) | −0.4(2) |
| Fe−C6 | 1.935(2) | 1.910(4) | 0.987(2) | −1.3(2) | 1.935(1) | 1.911(4) | 0.987(2) | −1.3(2) |
| C1−N1 | 1.156(2) | 1.158(5) | 1.002(5) | 0.2(5) | 1.159(2) | 1.149(5) | 0.992(5) | −0.8(5) |
| C2−N2 | 1.158(2) | 1.172(6) | 1.012(5) | 1.2(5) | 1.159(2) | 1.161(6) | 1.002(5) | 0.2(5) |
| C3−N3 | 1.158(2) | 1.179(6) | 1.018(5) | 1.8(5) | 1.154(2) | 1.177(5) | 1.020(5) | 2.0(5) |
| C4−N4 | 1.154(2) | 1.169(5) | 1.013(5) | 1.3(5) | 1.153(2) | 1.175(5) | 1.019(5) | 1.9(5) |
| C5−N5 | 1.160(2) | 1.161(5) | 1.001(5) | 0.1(5) | 1.159(2) | 1.156(5) | 0.997(5) | −0.3(5) |
| C6−N6 | 1.156(2) | 1.169(5) | 1.011(5) | 1.1(5) | 1.158(2) | 1.156(5) | 0.998(5) | −0.2(5) |
| X−N6 | 2.592(1) | 2.513(4) | 0.970(2) | −3.0(2) | 2.516(1) | 2.450(3) | 0.974(1) | −2.6(1) |
| X−O1 | 2.492(1) | 2.516(3) | 1.010(1) | 1.0(1) | 2.425(1) | 2.444(3) | 1.008(1) | 0.8(1) |
| X−O2 | 2.4826(10) | 2.468(2) | 0.994(1) | −0.6(1) | 2.413(1) | 2.402(3) | 0.996(1) | −0.4(1) |
| X−O3 | 2.512(1) | 2.506(3) | 0.998(1) | −0.2(1) | 2.4494(10) | 2.447(2) | 0.999(1) | −0.1(1) |
| X−O10 | 2.443(1) | 2.433(3) | 0.996(1) | −0.4(1) | 2.3869(10) | 2.382(3) | 0.998(1) | −0.2(1) |
| X−O20 | 2.462(1) | 2.477(4) | 1.006(2) | 0.6(2) | 2.3972(10) | 2.418(4) | 1.009(2) | 0.9(2) |
| X−O30 | 2.426(1) | 2.415(3) | 0.996(1) | −0.4(1) | 2.3685(10) | 2.361(3) | 0.997(1) | −0.3(1) |
| X−O40 | 2.466(1) | 2.563(4) | 1.039(2) | 3.9(2) | 2.4111(9) | 2.502(3) | 1.038(1) | 3.8(1) |
| | TbFeDMF(**5**) | | | | YbFeDMF(**6**) | | | |
| bond | ground state (Å) | excited state (Å) | ratio | change (%) | ground state (Å) | excited state (Å) | ratio | change (%) |
| Fe−C1 | 1.931(2) | 1.912(4) | 0.990(2) | −1.0(2) | 1.929(2) | 1.928(5) | 0.999(3) | −0.1(3) |
| Fe−C2 | 1.938(2) | 1.898(6) | 0.979(3) | −2.1(3) | 1.938(2) | 1.897(7) | 0.979(4) | −2.1(4) |
| Fe−C3 | 1.932(2) | 1.903(6) | 0.985(3) | −1.5(3) | 1.939(2) | 1.903(6) | 0.981(3) | −1.9(3) |
| Fe−C4 | 1.930(2) | 1.888(5) | 0.978(3) | −2.2(3) | 1.931(2) | 1.892(6) | 0.980(3) | −2.0(3) |


dx.doi.org/10.1021/ic2015258 |*Inorg. Chem.* 2011, 50, 10974–10984

**Table 2. Continued**

| | TbFeDMF(**5**) | | | | YbFeDMF(**6**) | | | |
|---|---|---|---|---|---|---|---|---|
| bond | ground state (Å) | excited state (Å) | ratio | change (%) | ground state (Å) | excited state (Å) | ratio | change (%) |
| Fe−C5 | 1.942(2) | 1.921(5) | 0.989(3) | −1.1(3) | 1.947(2) | 1.910(6) | 0.981(3) | −1.9(3) |
| Fe−C6 | 1.919(2) | 1.906(5) | 0.993(3) | −0.7(3) | 1.923(2) | 1.896(6) | 0.986(3) | −1.4(3) |
| C1−N1 | 1.156(3) | 1.140(6) | 0.986(6) | −1.4(6) | 1.157(3) | 1.119(6) | 0.967(6) | −3.3(6) |
| C2−N2 | 1.159(3) | 1.163(7) | 1.003(7) | 0.3(7) | 1.154(3) | 1.158(8) | 1.003(7) | 0.3(7) |
| C3−N3 | 1.162(3) | 1.163(7) | 1.001(7) | 0.1(7) | 1.152(3) | 1.151(7) | 0.999(7) | −0.1(7) |
| C4−N4 | 1.153(3) | 1.167(6) | 1.012(6) | 1.2(6) | 1.152(3) | 1.151(7) | 0.999(7) | −0.1(7) |
| C5−N5 | 1.161(3) | 1.170(6) | 1.008(6) | 0.8(6) | 1.156(3) | 1.167(7) | 1.010(7) | 1.0(7) |
| C6−N6 | 1.159(3) | 1.152(6) | 0.994(6) | −0.6(6) | 1.157(3) | 1.151(6) | 0.995(6) | −0.5(6) |
| X−N6 | 2.431(2) | 2.381(4) | 0.979(2) | −2.1(2) | 2.366(2) | 2.311(4) | 0.977(2) | −2.3(2) |
| X−O1 | 2.359(2) | 2.372(4) | 1.006(2) | 0.6(2) | 2.300(1) | 2.312(4) | 1.005(2) | 0.5(2) |
| X−O2 | 2.374(2) | 2.375(3) | 1.000(1) | 0.0(1) | 2.327(1) | 2.304(4) | 0.990(2) | −1.0(2) |
| X−O3 | 2.416(2) | 2.421(3) | 1.002(1) | 0.2(1) | 2.354(1) | 2.353(4) | 1.000(2) | 0.0(2) |
| X−O10 | 2.352(2) | 2.334(3) | 0.992(1) | −0.8(1) | 2.307(1) | 2.292(4) | 0.994(2) | −0.6(2) |
| X−O20 | 2.377(2) | 2.378(4) | 1.000(2) | 0.0(2) | 2.320(1) | 2.323(6) | 1.001(3) | 0.1(3) |
| X−O30 | 2.395(2) | 2.378(3) | 0.993(1) | −0.7(1) | 2.340(1) | 2.330(4) | 0.996(2) | −0.4(2) |
| X−O40 | 2.357(1) | 2.412(4) | 1.024(2) | 2.4(2) | 2.294(1) | 2.341(5) | 1.020(2) | 2.0(2) |

| | NdCoDMF (**7**) | | | |
|---|---|---|---|---|
| | GS (Å) | EXC (Å) | EXC/GS | change (%) |
| Co−C1 | 1.887(1) | 1.889(1) | 1.001(1) | 0.1(1) |
| Co−C2 | 1.891(1) | 1.892(1) | 1.001(1) | 0.1(1) |
| Co−C3 | 1.899(1) | 1.899(1) | 1(1) | 0(1) |
| Co−C4 | 1.891(1) | 1.893(1) | 1.001(1) | 0.1(1) |
| Co−C5 | 1.890(1) | 1.892(1) | 1.001(1) | 0.1(1) |
| Co−C6 | 1.892(1) | 1.892(1) | 1(1) | 0.0(1) |
| C1−N1 | 1.153(1) | 1.152(2) | 0.999(2) | −0.1(2) |
| C2−N2 | 1.157(2) | 1.154(2) | 0.997(2) | −0.3(2) |
| C3−N3 | 1.152(2) | 1.154(2) | 1.001(2) | 0.1(2) |
| C4−N4 | 1.147(1) | 1.147(2) | 0.999(2) | −0.1(2) |
| C5−N5 | 1.153(1) | 1.151(2) | 0.998(2) | −0.2(2) |
| C6−N6 | 1.155(1) | 1.154(2) | 0.999(2) | −0.1(2) |
| Nd−N6 | 2.5466(10) | 2.545(1) | 0.999(1) | −0.1(1) |
| Nd−O1 | 2.4609(8) | 2.4586(9) | 0.999(1) | −0.1(1) |
| Nd−O2 | 2.4458(8) | 2.4459(9) | 1.000(1) | 0.0(1) |
| Nd−O3 | 2.4705(8) | 2.4696(9) | 1.000(1) | 0.0(1) |
| Nd−O10 | 2.4120(8) | 2.4127(9) | 1.000(1) | 0.0(1) |
| Nd−O20 | 2.4294(8) | 2.4292(9) | 1.000(1) | 0.0(1) |
| Nd−O30 | 2.3938(8) | 2.3941(9) | 1.000(1) | 0.0(1) |
| Nd−O40 | 2.4300(8) | 2.4314(9) | 1.001(1) | 0.1(1) |

For all six Fe-containing complexes, it has been possible to determine the structure from the single crystal EXC data collections. In the case of NdCoDMF, no excited state structure could be separated and modeled, and the only effect of illumination was a very small increase in the thermal parameters—see Table 2 and Figure 7. This change is most likely attributed to a small heating effect caused by the UV laser. For all of the Fe compounds, the EXC data consist of a mixture of the ground state structure and excited state structure. Significant structural changes are observed in the excited state. The refined occupancies of the excited states are in the range 80−94%. The metal ligand and cyanide bond lengths in the excited states are plotted in Figures 4−6 for all of the Fe-containing compounds.

The same tendencies in bond length changes are generally present in the excited state for all Fe compounds. A large decrease is observed in Figure 6 for the Ln−N6 bonds, while the bonds to O40 increase between 2% and 4% in the excited state structure. More widespread fluctuations are, however, found in the bonds to the iron atoms. Significant decreases (up to 3%) are observed in the Fe−C bonds (Figure 4), while the corresponding cyanide bonds, C−N, increase in the excited state structures (Figure 5). Thus, the changes in C−N bonds are somehow correlated with the changes in the corresponding Fe−C bonds, and the largest changes are generally observed for the cyanide groups 1−3 in all excited state structures.

As illustrated in Figure 7, a significant increase in the atomic displacement parameters (ADPs) is observed in the excited state


dx.doi.org/10.1021/ic2015258 |*Inorg. Chem.* 2011, 50, 10974–10984

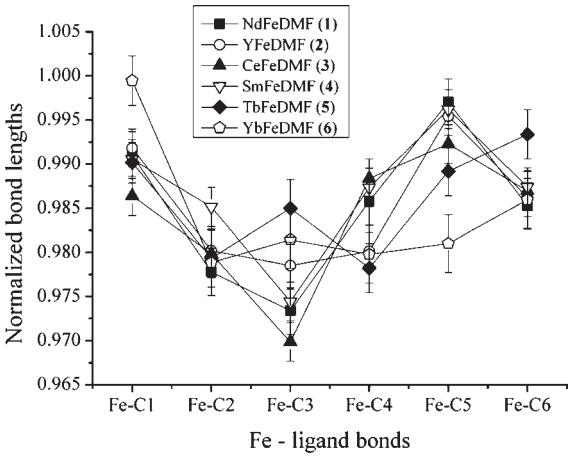


**Figure 4.** Fe−ligand bond lengths in the excited states of **1**−**6** normalized to the ground state values.

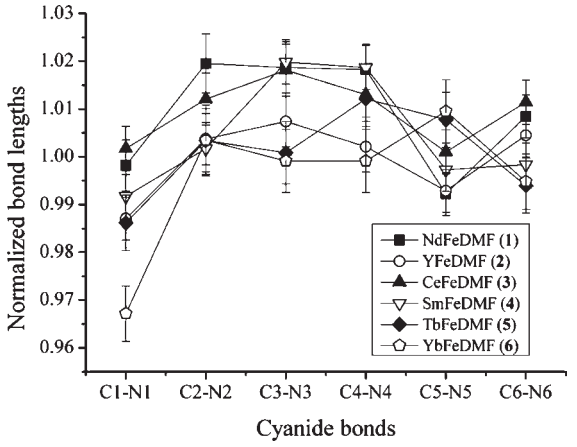


**Figure 5.** Cyanide ligand bond lengths in the excited states of **1**−**6** normalized to the ground state values.

structures measured during continuous UV irradiation. Especially DMF groups 20 and 40 and the solvent water molecule experience a large increase in ADPs in the excited state. The large ADPs may be a sign of structural disorder in these groups; however, it has not been possible to refine such disorder in the excited state structure. Besides these DMF groups, there is a large, but fairly uniform, increase in the ADPs on all other atoms. No clear explanation exists for this observation, but it is noteworthy that it is observed for all of the Fe compounds while the Co compound is not affected similarly. Other photocrystallographic studies have reported similar large increases in the ADPs in the excited state.[14,22,23,33] Several effects could contribute to the large increase in ADPs such as heating or radiation damage from the laser or the presence of several metastable states with small differences in their nuclear configurations. The relatively large decrease in unit cell volumes contradict, however, the possibilities of a heating or radiation damage effect, as both of these would normally lead to an expansion of the cell.[34,35] It has previously been reported that NdFeDMF (**1**) does not suffer from radiation damage from X-rays.[22] Furthermore, radiation damage is expected to induce random disorder and not clear systematic changes as observed for the Fe crystals in the excited

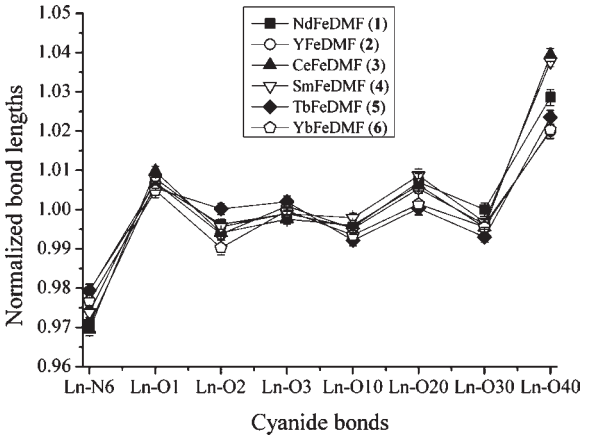


**Figure 6.** Lanthanide ligand bond lengths in the excited states of **1**−**6** normalized to the ground state values.

states. The clear changes observed in the excited state structure are thus expected to be a consequence of the photoexcitation.

The general trends in structural changes observed in the excited state structure of NdFeDMF for the synchrotron experiments are in good agreement with the previously reported structure.[22] Thus, it is possible to obtain similar results both in two different single crystal experiments as well as in a powder diffraction experiment despite the different nature of the experiments. This confirms an excitation of NdFeDMF upon UV illumination.

The volume of the crystal used at the synchrotron is almost 3 orders of magnitude smaller compared to the one used in the conventional X-ray experiment. This explains the much shorter time scale observed for the structural changes reported here compared with the previous conventional experiment. However, the unit cell decrease of NdFeDMF (**1**; 1.3%) is not as large here as previously obtained in the laboratory experiment, where a decrease of 1.7% was observed.[22] The bond length changes were also larger in the home laboratory experiment, while the refined occupancy of the excited state was smaller, 0.786(1) for the laboratory data compared to 0.861(2) for the synchrotron data. We expect that the change in cell volume reflects the amount of excitation induced in the compound. The fact that the ground state and excited state structures are difficult to resolve induces a correlation between the geometry of the excited state structure and the occupancy parameter. The largest correlations (less than 80%) are found between the occupancy and the Nd atomic parameters in the excited state. Thus, the large ADPs are unlikely to be a consequence of an overestimation of the occupancy parameter. Nevertheless, if an excited state with more pronounced bond length changes is held fixed in the refinement of the synchrotron data, a smaller occupancy of the excited state is also expected. The use of smaller crystals should in principle increase the degree of excitation, as the UV light is more likely to penetrate the entire sample. However, the two types of experiments differ not only in type of X-ray radiation but also in the UV light source used for excitation. There is a difference both in wavelength and intensity of the UV light, and this presumably causes the observed different amounts of excitation.

The decrease in cell volume of NdFeDMF (**1**) of only 1.3% obtained from PXRD is lower than the conventional single crystal results (1.7%). If we correlate the volume change of 1.3% to a degree of excitation from the laboratory single crystal values, we arrive at a value for the degree of excitation of

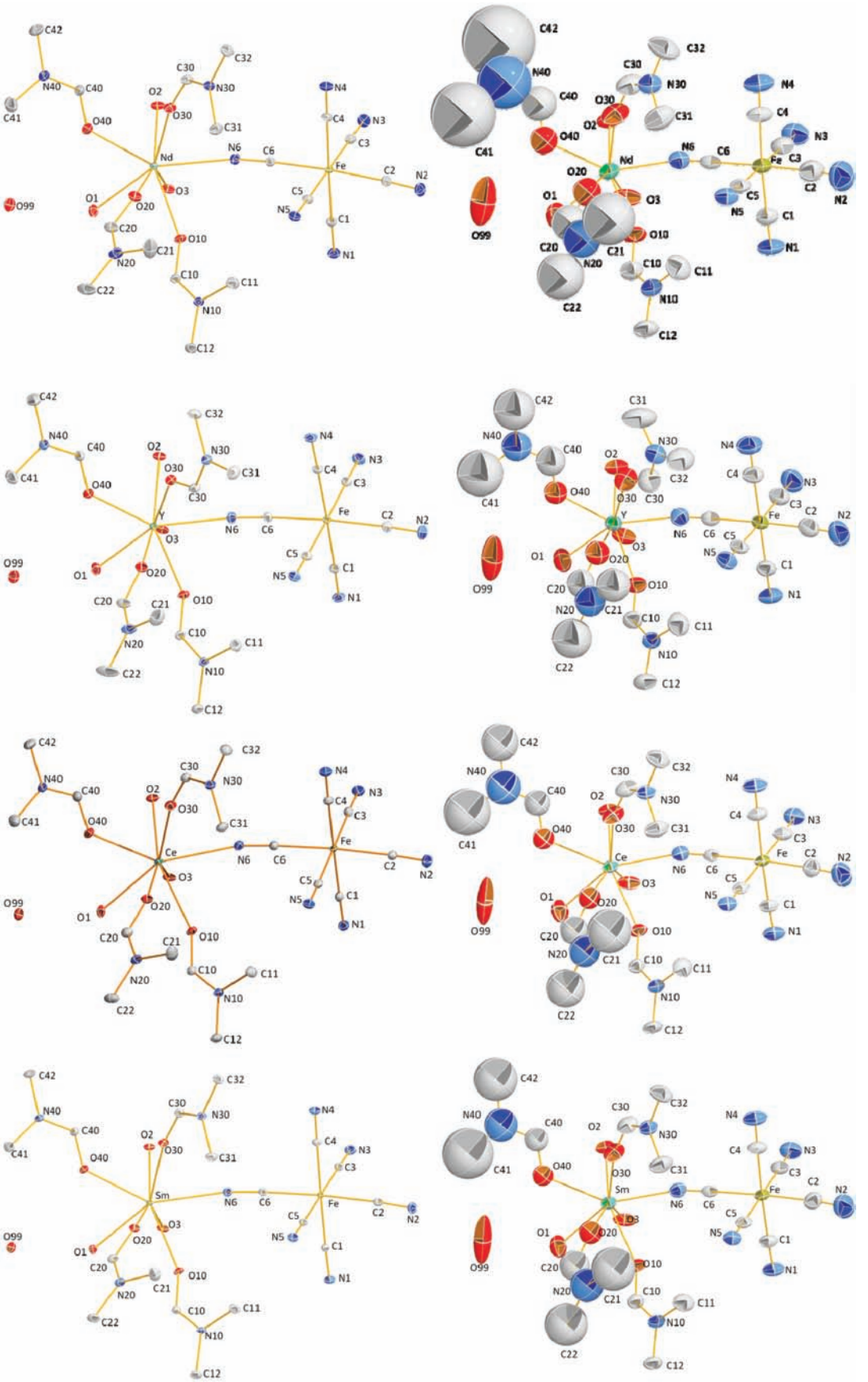


**Figure 7.** Continued


dx.doi.org/10.1021/ic2015258 |*Inorg. Chem.* 2011, 50, 10974–10984

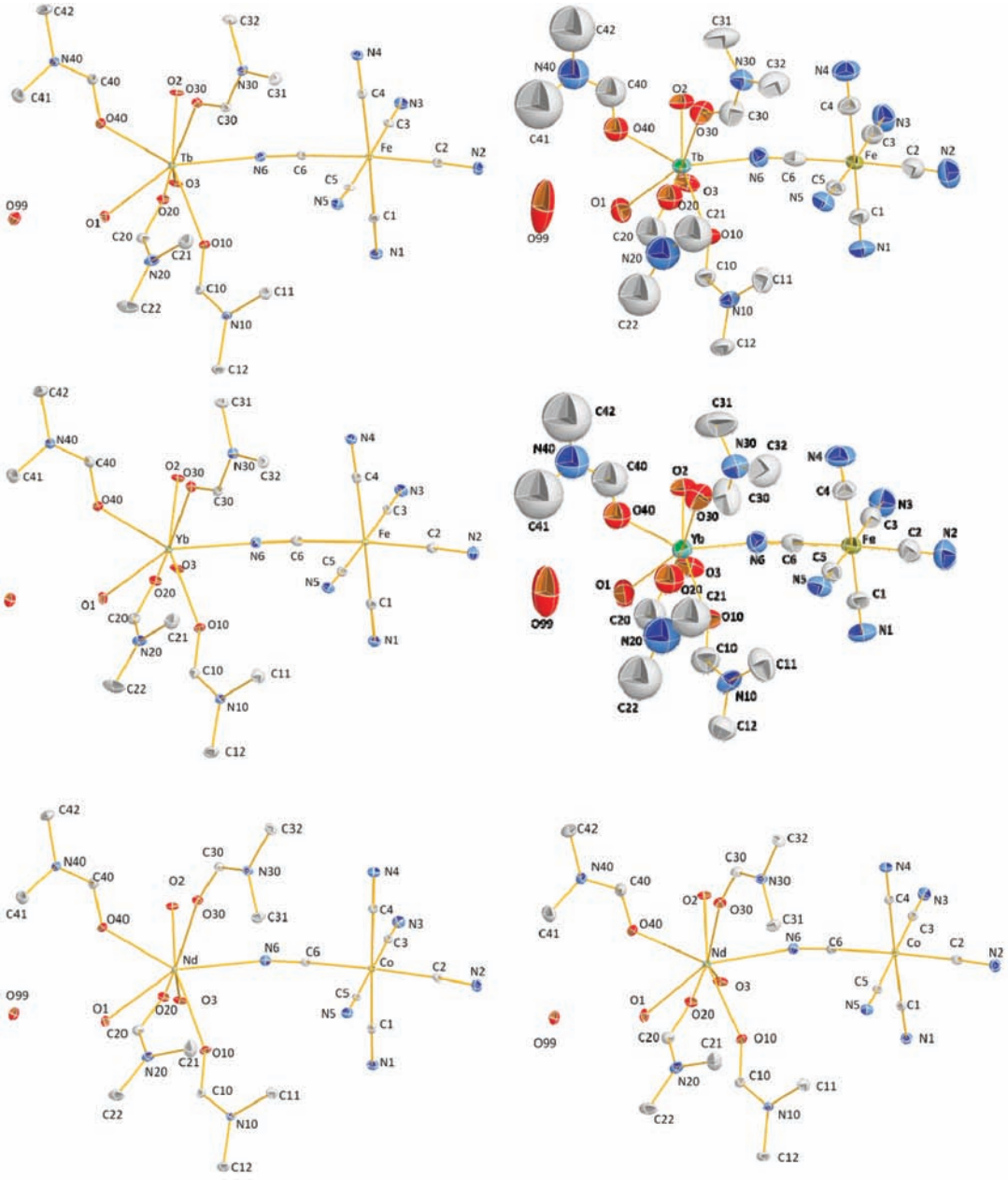


**Figure 7.** The ground state (left) and excited state (right) structures of **1**−**7** with atomic displacement ellipsoids drawn at the 50% probability level. H atoms are omitted for clarity.

less than 80%.[22] It therefore appears very difficult to increase the amount of excitation by using smaller crystallites, which again suggests that it is not possible to fully excite NdFeDMF (**1**) using the current experimental setup.

In order to determine the influence of the 4f metal on the excitation process, powder X-ray diffraction data with simultaneous UV illumination have been measured for $K_3Fe(CN)_6$, which consists of isolated $Fe(CN)_6^{3-}$ entities, thereby resembling one-half of the bimetallic compounds studied here. The unit cell volume of this compound as a function of time after the UV light has been turned on is shown in Figure 8, showing only a small increase in the unit cell parameters and thereby indicating that a minor heating effect is the result of the UV light while no photoexcitation takes place for this compound. Structural changes are thus only observed in compounds containing both an $Fe(CN)_6^{3-}$ entity and a 4f metal, and somehow the excitation process therefore must be dependent on the simultaneous presence of both metal centers.

Parallel to the photocrystallographic studies, photomagnetic investigations were performed on NdFeDMF (**1**) and LaFeDMF (**9**). The normalized magnetic responses are shown in Figures 9 and 10 for **1** and **9**, respectively, upon UV light illumination at 10 K.

At 10 K under UV light illumination, an increase is observed in the magnetic response of the powder sample of NdFeDMF (**1**). However, the increase of the magnetic signal represents less than 3%, while 45% has been previously reported.[21] Several unsuccessful attempts were made to increase the photomagnetic


dx.doi.org/10.1021/ic2015258 |*Inorg. Chem.* 2011, 50, 10974–10984

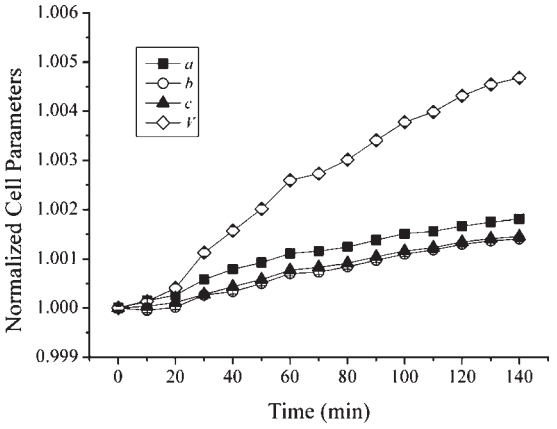


**Figure 8.** Unit cell volume of $K_3Fe(CN)_6$ (**8**) as a function of time determined by powder X-ray diffraction at 15 K. The laser is turned on immediately after $t = 0$ min. The esd's are smaller than the symbols used in the plot.

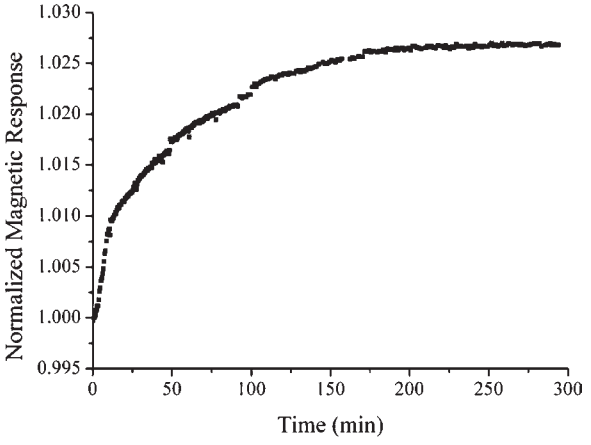


**Figure 9.** The normalized magnetic response of NdFeDMF (**1**) as a function of time at $H = 5000$ G. The UV light is turned on immediately after $t = 0$ min.

response by varying, e.g., the laser intensity, the magnetic field, the temperature, the amount of sample, and the crystallite sizes. In each case, the efficiency of the photoexcitation was not improved. It seems that, as also noticed by Li,[36] the efficiency of the photoexcitation appears to be linked to the sample preparation. Nevertheless, despite an increase of less than 3%, a clear photomagnetic effect is observed on our powder sample of NdFeDMF (**1**). Moreover, the result is not linked to any artificial thermal treatment. When the photosaturation is reached and the UV irradiation stopped, the magnetic signal remains relatively stable; i.e., at 25 K, a decrease of less than 0.3% is observed after 2 h of relaxation.

A similar photomagnetic effect, associated with an increase in magnetization, is also observed for compound **9** when the sample is illuminated with UV light. However, as in the case of NdFeDMF (**1**), the effect is small (1%) but significant. We have previously reported that this compound shows similar structural changes to those of NdFeDMF (**1**) upon UV illumination,[23] and therefore the combined results from the photomagnetic measurements and the photocrystallographic experiments indicate that the increase in magnetization of the excited state (of **1**) is

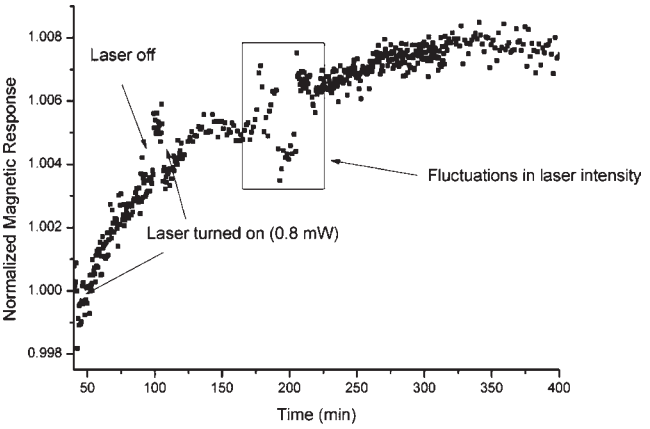


**Figure 10.** The normalized magnetic response of LaFeDMF (**9**) as a function of time at $H = 10\,000$ G.

related to the structural changes observed in the excited state. Since for all of the following compounds LnFeDMF, Ln = Y, La, Ce, Nd, Sm, Gd, Tb, and Yb, similar structural changes are observed upon UV illumination and the only complex belonging to this structure family not responding to UV light is NdCoDMF, the photomagnetic measurements suggest that the entire series of isostructural complexes exhibits similar magnetic responses in the UV-induced excited state crystal structure. We thus anticipate that the same mechanism is involved in the excitation process for all of the iron-containing complexes. Thus, the iron atom and the cyanide ligands must play an essential role in the excitation, in which the choice of the lanthanide ion is secondary. Nevertheless, the presence of the lanthanide atom is essential. As an extension to this effect, we have examined the importance of the nature of the chemical bridge between the iron and rare earth atoms in a study of NdFeDMA in which the metal sites are not covalently connected through a cyano bridge.[24] For this compound, a decrease in the unit cell was also observed along with significant structural changes, strongly indicating that NdFeDMA is photoactive upon UV irradiation in a similar way to the DMF analogues.

From theoretical analysis of NdFeDMF, it has been shown that charge transfer from the cyanide ligands to the lanthanide atoms may explain the photomagnetic effect in good agreement with the observed structural changes.[23] The charge transfer is mainly taking place from the cyanide ligands in agreement with the increased cyanide bond lengths and shorter Fe−C bond lengths. The theoretical analysis indicates that charge is moved from the cyanide ligands to the 4f metal center, but to a first approximation the charge density around the Fe atom is not affected. This hypothesis does therefore not contradict earlier Mössbauer results in the excited state, which showed only subtle differences in the density on Fe in the excited state of NdFeDMF.[21] Even though the theoretical calculations were focused on NdFeDMF, it is anticipated that the isostructural complexes have similar charge transferabilities in the same energy range, as the lanthanide atom is not expected to have much influence on the molecular orbitals around the iron atom. This indicates that all LnFeDMF compounds will show changes in their magnetic moment upon excitation due to more unpaired spins in the cyanide ligands and on the lanthanide atom.


dx.doi.org/10.1021/ic2015258 |*Inorg. Chem.* 2011, 50, 10974–10984

## CONCLUSION

We have shown that the structural changes in all of the present Fe-containing 3d−4f bimetallic complxes are very similar and in good agreement with previous results, despite coming from two different experimental setups. Thus, the Fe−ligand bond lengths decrease while the cyanide bond lengths increase. By studying the isolated octahedral $Fe(CN)_6$ anions as present in $K_3Fe(CN)_6$, we have shown that these entities on their own are not excited in the solid state by UV light illumination. This indicates that the structural changes are a result of a cooperative effect involving both the transition metal and the lanthanide, as also suggested by theoretical calculations.

The measured cell volume changes in the synchrotron PXRD excited state measurements, which indicates that the excitation rate is not increased despite the use of much smaller crystallites. The present study has provided abundant evidence that the increase in magnetization upon UV illumination is much smaller, by a factor of about 15, compared with previously reported data.

## ASSOCIATED CONTENT

**Supporting Information.** X-ray crystallographic CIF file for **1**−**7**. This material is available free of charge via the Internet at http://pubs.acs.org.

## AUTHOR INFORMATION

**Corresponding Author**
*E-mail: bo@chem.au.dk.

## ACKNOWLEDGMENT

The study was supported by the Danish National Research Foundation (CMC), The Danish Strategic Research Council (CEM), The Danish Research Council for Nature and Universe (Danscatt), the GIS-Advanced Materials in Aquitaine (AMA), and the Aquitaine Region through the development of the ICPA platform at the ICMCB: International Center of Photomagnetism in Aquitaine. Synchrotron radiation experiments were performed at BL44B2 in SPring-8 with the approval of RIKEN (Proposal No. 20100049). ChemMatCARS Sector 15 is principally supported by the National Science Foundation/Department of Energy under grant number NSF/CHE-0822838. Use of the Advanced Photon Source was supported by the U.S. Department of Energy, Office of Science, Office of Basic Energy Sciences, under Contract No. DE-AC02-06CH11357.

## REFERENCES

(1) Coppens, P.; Novozhilova, I.; Kovalevsky, A. *Chem. Rev.* **2002**, *102*, 861–883.
(2) Coppens, P. *Chem. Commun.* **2003**, 1317–1320.
(3) Cole, J. M. *Acta Crystallogr., Sect. A: Found. Crystallogr.* **2008**, *64*, 259–271.
(4) Ichiyanagi, K.; Hebert, J.; Toupet, L.; Cailleau, H.; Guionneau, P.; Létard, J. F.; Collet, E. *Phys. Rev. B: Condens. Matter Mater. Phys.* **2006**, *73*, 060408.
(5) Legrand, V.; Pillet, S.; Carbonera, C.; Souhassou, M.; Létard, J. F.; Guionneau, P.; Lecomte, C. *Eur. J. Inorg. Chem.* **2007**, 5693–5706.
(6) Cole, J. M. *Z. Kristallogr.* **2008**, *223*, 363–369.
(7) Bowes, K. F.; Cole, J. M.; Husheer, S. L. G.; Raithby, P. R.; Savarese, T. L.; Sparkes, H. A.; Teat, S. J.; Warren, J. E. *Chem. Commun.* **2006**, 2448–2450.
(8) Rudlinger, M.; Schefer, J.; Vogt, T.; Woike, T.; Haussuhl, S.; Zollner, H. *Physica B* **1992**, *180*, 293–298.
(9) Carducci, M. D.; Pressprich, M. R.; Coppens, P. *J. Am. Chem. Soc.* **1997**, *119*, 2669–2678.
(10) Kovalevsky, A. Y.; Bagley, K. A.; Coppens, P. *J. Am. Chem. Soc.* **2002**, *124*, 9241–9248.
(11) Kovalevsky, A. Y.; Bagley, K. A.; Cole, J. M.; Coppens, P. *Inorg. Chem.* **2003**, *42*, 140–147.
(12) Kusz, J.; Spiering, H.; Gutlich, P. *J. Appl. Crystallogr.* **2001**, *34*, 229–238.
(13) Huby, N.; Guerin, L.; Collet, E.; Toupet, L.; Ameline, J. C.; Cailleau, H.; Roisnel, T.; Tayagaki, T.; Tanaka, K. *Phys. Rev. B: Condens. Matter Mater. Phys.* **2004**, *69*, 020101.
(14) Pillet, S.; Legrand, V.; Weber, H. P.; Souhassou, M.; Létard, J. F.; Guionneau, P.; Lecomte, C. *Z. Kristallogr.* **2008**, *223*, 235–249.
(15) Trzop, E.; Cointe, M. B. L.; Cailleau, H.; Toupet, L.; Molnar, G.; Bousseksou, A.; Gaspar, A. B.; Real, J. A.; Collet, E. *J. Appl. Crystallogr.* **2007**, *40*, 158–164.
(16) Kim, C. D.; Pillet, S.; Wu, G.; Fullagar, W. K.; Coppens, P. *Acta Crystallogr., Sect. A: Found. Crystallogr.* **2002**, *58*, 133–137.
(17) Ozawa, Y.; Terashima, M.; Mitsumi, M.; Toriumi, K.; Yasuda, N.; Uekusa, H.; Ohashi, Y. *Chem. Lett.* **2003**, *32*, 62–63.
(18) Yasuda, N.; Kanazawa, M.; Uekusa, H.; Ohashi, Y. *Chem. Lett.* **2002**, 1132–1133.
(19) Collet, E.; Lemee-Cailleau, M. H.; Buron-Le Cointe, M.; Cailleau, H.; Wulff, M.; Luty, T.; Koshihara, S. Y.; Meyer, M.; Toupet, L.; Rabiller, P.; Techert, S. *Science* **2003**, *300*, 612–615.
(20) Coppens, P. *J. Phys. Chem. Lett.* **2011**, *2*, 616–621.
(21) Li, G. M.; Akitsu, T.; Sato, O.; Einaga, Y. *J. Am. Chem. Soc.* **2003**, *125*, 12396–12397.
(22) Svendsen, H.; Overgaard, J.; Chevallier, M.; Collet, E.; Iversen, B. B. *Angew. Chem., Int. Ed.* **2009**, *48*, 2780–2783.
(23) Svendsen, H.; Overgaard, J.; Chevallier, M. A.; Collet, E.; Chen, Y.-S.; Jensen, F.; Iversen, B. B. *Chem.—Eur. J.* **2010**, *16*, 7215–7223.
(24) Svendsen, H.; Overgaard, J.; Chen, Y.-S.; Iversen, B. B. *Chem. Commun.* **2011**, *47*, 9486–9488.
(25) Li, G. M.; Sato, O.; Akitsu, T.; Einaga, Y. *J. Solid State Chem.* **2004**, *177*, 3835–3838.
(26) Li, G. M.; Yan, P. F.; Sato, O.; Einaga, Y. *J. Solid State Chem.* **2005**, *178*, 36–40.
(27) Hardie, M. J.; Kirschbaum, K.; Martin, A.; Pinkerton, A. A. *J. Appl. Crystallogr.* **1998**, *31*, 815–817.
(28) Sheldrick, G. M. *SAINT+*; *SADABS*; *XPREP*; *SHELXTL* (programs included in the Bruker SMART CCD software); Bruker: Madison, WI, 2003.
(29) Blessing, R. H. *J. Appl. Crystallogr.* **1997**, *30*, 421–426.
(30) Kato, K.; Hirose, R.; Takemoto, M.; Ha, S.; Kim, J.; Higuchi, M.; Matsuda, R.; Kitagawa, S.; Takata, M. *AIP Conf. Proc.* **2010**, *1234*, 875–878.
(31) Nishibori, E.; Sunaoshi, E.; Yoshida, A.; Aoyagi, S.; Kato, K.; Takata, M.; Sakata, M. *Acta Crystallogr., Sect. A: Found. Crystallogr.* **2007**, *63*, 43–52.
(32) Rodriguez-Carvajal, J. *FullProf*; Laboratoire Léon Brillouin (CEA-CNRS): Gif-sur-Yvette Cedex, France.
(33) Warren, M. R.; Brayshaw, S. K.; Johnson, A. L.; Schiffers, S.; Raithby, P. R.; Easun, T. L.; George, M. W.; Warren, J. E.; Teat, S. J. *Angew. Chem., Int. Ed.* **2009**, *48*, 5711–5714.
(34) Garman, E. F. *Acta Crystallogr., Sect. D: Biol. Crystallogr.* **2010**, *66*, 339–351.
(35) Meents, A.; Wagner, A.; Schneider, R.; Pradervand, C.; Pohl, E.; Schulze-Briese, C. *Acta Crystallogr., Sect. D: Biol. Crystallogr.* **2007**, *63*, 302–309.
(36) Li, G. M. Private communication.